7. CONCLUDING REMARKS

Clustered impacts result in craters and processes that depart significantly from single-body or two-body impacts. The observed differences provide new clues for understanding secondary cratering processes and low-strength/low-density impacts in general. The following list summarizes the more significant experimental results with applications to planetary processes.

1. Clustered impacts displace 5–10 times less mass than does a single impact of the same mass. This reduction in cratering efficiency has important implications for predicting the relative contribution of local and primary materials from secondary cratering. It also underscores the difficulty in estimating ejecta sizes from observed secondary craters.

2. Crater morphology is strongly dependent on the size and velocity of a cluster as well as the relative density and strength between the target and projectile. Crater floors were produced ranging from "flat" (with an incipient multiring pattern) to mounded to bowl-shaped. The crater rims are typically high in relief relative to their diameter, and the ejecta thins rapidly from the rim. These morphologies characterize lunar and Martian secondary craters and certain craters on Enceladus.

3. Oblique impacts of clustered projectiles consistently produce an ensemble of V-shaped ridges whose apex angle depends on the cluster dispersion and impact angle. Secondary craters commonly display V-shaped ridges (the herringbone pattern) and the experimental results are consistent with impact angles close to 45°.

4. Clustered vertical impacts produce an amorphous cloud at early times that evolves at later times into the well-defined (classic) single-body ejecta plume. The ejecta plume becomes gradually more inclined from the horizontal until at late times it resembles the plume produced by a single impactor. Clustered oblique impacts develop an equally distinctive low-angle ejecta plume with little uprange deposits. The evolution of the ejecta plume should enhance ejecta flow around large impact craters.

5. Clustered oblique impacts do not form the distinctive butterfly pattern of a single-body impact but form a fan-shaped pattern extending downrange. This unique pattern may help in identifying large basin secondaries. It also contributes to the formation of crater rays.

6. Projectile material from a clustered impact largely remains on the surface: contained by the crater in vertical impacts and strewn downrange in oblique impacts. The combination of projectile disperson, reduced cratering efficiency, and the downrange fan-shaped distribution may help explain variations in the albedo and spectral signature of primary material.

Preliminary results at very high impact velocities (>6 km/s) reveal both similar and strikingly different phenomena [*Schultz and Gault*, 1983]. We strongly suspect that craters below a certain size on the Earth and Venus may be very different from comparable size craters on the Moon owing to atmospheric breakup, as suggested by *Melosh* [1981]. Detailed comparisons and discussions will be forthcoming in a future contribution.

APPENDIX

For impact velocities higher than 1 km/s, clusters were produced by fragmenting pyrex spheres as they passed through thin aluminum foil (1–2 km/s) or paper (>3 km/s). The lateral dispersion of the pyrex fragments is largely due to centrifugal force resulting from spin on the projectile during launch. Two methods were used to calibrate the lateral dispersion and overall cluster configuration at impact. The first method employed aluminum witness plates placed at the target; the second used high frame rate overhead views that record the first contact at the target surface. Figure A1 illustrates a typical result for hypervelocity fragments impacting an aluminum witness plate. Each cluster displays a relatively well-contained pattern with uniform distribution of fragment sizes. The size distribution of holes in the witness plate is shown in Figure A2. No systematic attempt has been made to translate the size distribution of the holes to actual fragment size except to note that an unbroken 0.635-cm pyrex sphere at about the same velocity produces a 0.85-cm hole in a witness plate of the same thickness (0.09 cm). Thus the size of the holes will approximate the size of the fragments for sufficiently large fragments. The cumulative size distribution in Figure A2 indicates that about

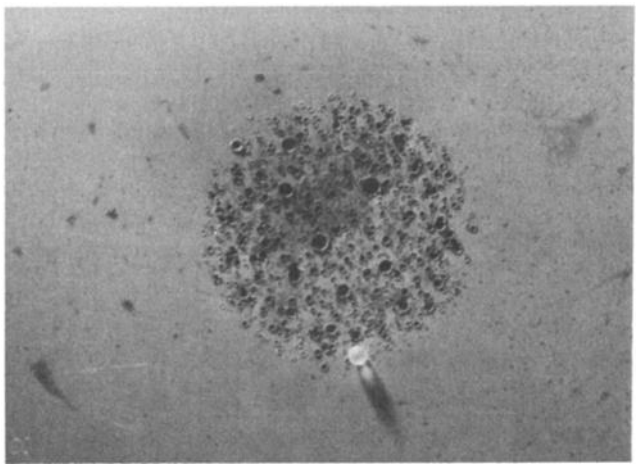

Fig. A1. Spatial distribution of pits produced by pyrex fragments impacting an aluminum witness plate. Pyrex fragments were created as a 0.635-cm pyrex sphere passed through a thin piece of paper at 5.5 km/s. Original size of pyrex shown at edge of cluster.

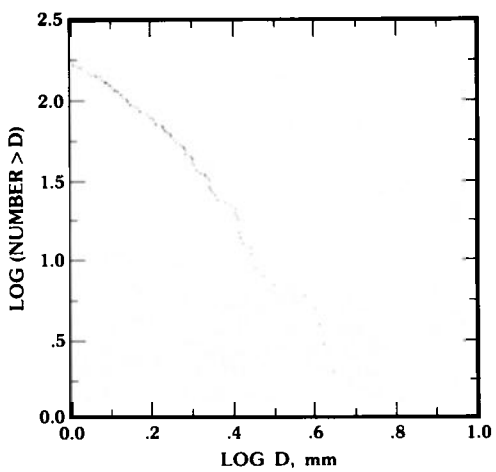

Fig. A2. Cumulative size distribution of holes created by shattered pyrex as shown in Figure A1. Falloff at sizes smaller than 1 mm largely reflects fragments unable to penetrate 0.09-cm-thick aluminum witness plate.